

Article

# Green Synthesised Silver Nanoparticles Using *Anoectochilus elatus* Leaf Extract: Characterisation and Evaluation of Antioxidant, Anti-Inflammatory, Antidiabetic, and Antimicrobial Activities

Bhuvaneshwari Venkataesan Kumari <sup>1</sup>, Renuka Mani <sup>2</sup>, Balakrishnan Ramajayam Asokan <sup>3</sup> ,  
Karthikeyan Balakrishnan <sup>4</sup> , Arulmani Ramasamy <sup>5</sup>, Rengasamy Parthasarathi <sup>6</sup>, Chitra Kandasamy <sup>7</sup>,  
Rubalakshmi Govindaraj <sup>8</sup>, Natesan Vijayakumar <sup>1,\*</sup>  and Sekar Vijayakumar <sup>9,\*</sup> 

- <sup>1</sup> Department of Biochemistry and Biotechnology, Faculty of Science, Annamalai University, Annamalainagar 608002, Tamil Nadu, India; bhuvibhuvi444@gmail.com
- <sup>2</sup> Department of Biochemistry, Periyar University, Salem 636011, Tamil Nadu, India; rrenuka43@gmail.com
- <sup>3</sup> Department of Pharmacology, Aarupadai Veedu Medical College & Hospital, Vinayaga Mission Research Foundation, Pondicherry 607403, Tamil Nadu, India; asokan.br@avmc.edu.in
- <sup>4</sup> Department of Chemistry, Faculty of Science, Annamalai University, Annamalainagar 608002, Tamil Nadu, India; bkarthikeyan863@gmail.com
- <sup>5</sup> Department of Chemistry, Government Arts College, C-Mutlur, Chidambaram 608102, Tamil Nadu, India; arulmanichezhian15@gmail.com
- <sup>6</sup> Department of Microbiology, Faculty of Agriculture, Annamalai University, Annamalainagar 608002, Tamil Nadu, India; parthaskeshore@gmail.com
- <sup>7</sup> Department of Biotechnology, Muthayammal College of Arts & Science, Rasipuram 637408, Tamil Nadu, India; chitramuthu156@gmail.com
- <sup>8</sup> GRD Bioclinical Research, Rasipuram, Namakkal 637401, Tamil Nadu, India; grdresearch@gmail.com
- <sup>9</sup> Marine College, Shandong University, Weihai 264209, China
- \* Correspondence: nv12507@annamalaiuniversity.ac.in (N.V.); vijaysekar05@gmail.com (S.V.)



**Citation:** Venkataesan Kumari, B.; Mani, R.; Asokan, B.R.; Balakrishnan, K.; Ramasamy, A.; Parthasarathi, R.; Kandasamy, C.; Govindaraj, R.; Vijayakumar, N.; Vijayakumar, S. Green Synthesised Silver Nanoparticles Using *Anoectochilus elatus* Leaf Extract: Characterisation and Evaluation of Antioxidant, Anti-Inflammatory, Antidiabetic, and Antimicrobial Activities. *J. Compos. Sci.* **2023**, *7*, 453. <https://doi.org/10.3390/jcs7110453>

Academic Editor: Francesco Tornabene

Received: 10 October 2023  
Revised: 20 October 2023  
Accepted: 30 October 2023  
Published: 1 November 2023



**Copyright:** © 2023 by the authors. Licensee MDPI, Basel, Switzerland. This article is an open access article distributed under the terms and conditions of the Creative Commons Attribution (CC BY) license (<https://creativecommons.org/licenses/by/4.0/>).

**Abstract:** The present study investigates the green synthesis of silver nanoparticles was carried out using a leaf extract of *Anoectochilus elatus* (*Ae*-AgNPs). The synthesised *Ae*-AgNPs were characterised using different analytical techniques like UV-visible spectroscopy, X-ray diffraction (XRD), Fourier transform infrared (FTIR), and scanning electron microscopy (SEM) with energy-dispersive X-ray analysis (EDX). Additionally, in vitro activities were investigated, and they possess antioxidant, anti-inflammatory, antidiabetic, and antimicrobial properties. The UV-Vis spectra exhibited characteristic absorption peaks at approximately 480 nm. FTIR identified functional groups of the *Ae*-AgNPs. The crystalline structure of the *Ae*-AgNPs was verified via XRD analysis. SEM studies revealed that the nanoparticles exhibited a spherical morphology. The fabrication of *Ae*-AgNPs was established by the EDX spectrum, which exhibited prominent signals of silver atoms. The *Ae*-AgNPs show potent antioxidant, anti-inflammatory, and antidiabetic activity compared to standard drugs. In addition, *Ae*-AgNPs demonstrated the most significant zone of Inhibition. This study affirms the superior biological capability of *Ae*-AgNPs for target drug delivery and their potential for usage in biomedical research and therapeutics.

**Keywords:** *Anoectochilus elatus*; antimicrobial activity; antioxidant; anti-inflammatory; silver nanoparticles

## 1. Introduction

*Anoectochilus elatus* (*Ae*), also known as the South Indian jewel orchid, Chinese ever-green orchid, or the King of Medicine, is a fascinating species of orchid found in tropic and subtropic climates. This plant is a member of the *Orchidaceae* family, which comprises over 2000 distinct orchid species. Originating in China and India and spreading over South and Southeast Asia to Australia and the southwest Pacific islands [1,2], this plant is well known

for its unique leaves and attractive blooms. The *Ae* is highly valued for its ornamental elegance and striking appearance, with its dark green leaves enriched with metallic silver or gold spots which makes it a highly regarded species among orchid enthusiasts. The *Ae* has a rich historical background in embracing ancient therapeutic traditions in Asian regions such as China, Taiwan, and Japan [3]. Therefore, due to the loss of their native habitats and the conversion of forests into agricultural lands, we saw during our numerous field trips to the Kolli Hills in the Eastern Ghats of Tamil Nadu that the spread of *Ae* populations was severely constrained [4,5]. The medicinal properties of the *Ae* are harnessed from different plant components, including leave, stems, and roots. One of the notable characteristics of *Ae* is its rich content of bioactive compounds, including flavonoids, phenolic, and polysaccharides, which contribute to the plant's therapeutic potential [4–7]. Historically, it has been used to treat a wide range of medical conditions, including liver illness, respiratory trouble, and gastrointestinal disorders. The plant has also been used to support cardiovascular health and anticancer properties. Recent studies have shown that certain compounds in the orchid exhibit anti-tumour effects and may help inhibit the growth of cancer cells [7].

The World Health Organization recommends traditional medicine because of its efficacy and safety. In recent years, there has been a growing concern about the environmental impact of conventional synthesis methods for nanoparticles [8,9]. As a result, researchers have turned their attention toward developing environmentally friendly approaches, such as green synthesis, to produce nanoparticles. One of the most extensively studied examples of green synthesis is the production of silver nanoparticles [10,11]. Additionally, it has been observed that biosynthesised silver nanoparticles have a variety of uses in biomedical sciences. Various natural compounds have been utilised for the biogenesis of silver nanoparticles in this context [12]. A better reducing natural substance is constantly sought to make stable, extensively effective silver nanoparticles. Additionally, natural products play a significant role in the traditional medical system for maintaining human health and treating disorders [13]. Flavonoids, tannins, terpenoids, and alkaloids are a few secondary metabolites of plants that have been studied for their potential as drugs in vitro.

The conventional medical system has used *Ae* species to treat hypertension and pulmonary, hepatic, chest, and digestive disorders [14]. In light of this, species with both therapeutic and aesthetic value are required. To synthesise, characterise, and assess the antioxidant, anti-inflammatory, antidiabetic, and antibacterial effects of AgNPs using *Ae* leaf extract, we devised this research.

## 2. Materials and Methods

### 2.1. Chemicals

Silver nitrate, dimethyl sulphoxide, sodium hydroxide, trichloroacetic acid, ascorbic acid, DPPH, acarbose, aspirin, hydrogen peroxide, and microbiological media were procured from Otto Chemical-Mumbai. In this investigation, all the solutions were made using deionised water. All additional chemicals and reagents were of very high analytical purity.

### 2.2. Confirmation of Plant Materials

*Anoectochilus elatus* leaves were collected from Kolli Hills in Tamil Nadu, India. To accurately identify the leaves, they were examined in collaboration with Dr. P. Jayaraman, an expert from the Plant Anatomy Research Institute located in West Tambaram, Chennai, India. A herbarium sample was meticulously prepared, assigned a unique registration number, and precisely determined by Dr. P. Jayaraman (PARC/2022/4766 certificate). An amount of 10 g of finely engraved dried leaves of *Anoectochilus elatus* was subjected to boiling in 100 mL of distilled water at 60 °C for approximately 10 min and then cooled at ambient temperature. The solution underwent filtration using Whatman No. 1 to eliminate particulate matter, ensuring the acquisition of accurate solutions. Subsequently, these precise solutions were refrigerated at 4 °C in 250 mL Erlenmeyer flasks to facilitate further experimentation.

### 2.3. Bio-Inspired Synthesis of AgNPs

The bio-inspired synthesis of AgNPs was performed with a 50 mM aqueous solution composed of AgNO<sub>3</sub> prepared by dissolving 8.4 g of AgNO<sub>3</sub> in 1000 mL of distilled water [15]. Then, 20 mL of the prepared plant extract was mixed with 80 mL of the 50 mM aqueous salt solution. The reaction mixture was kept for 2 h at room temperature, and the transformation of the colourless solution into a dark brown material demonstrated that AgNPs were created during the reduction of AgNO<sub>3</sub> [16]; the suspension was subjected to centrifugation at 10,000 rpm for 25 min. The resultant pellet, which included *Ae*-AgNPs, underwent meticulous cleaning before being dried at 65 °C overnight.

### 2.4. Characterisation of *Ae*-AgNPs

#### 2.4.1. UV-Vis Analysis

To confirm the *Ae*-AgNPs formation, UV-Vis analysis was conducted utilising a Shimadzu spectrophotometer (Japan, Kyoto, Shimadzu) as described in the study by [17]. The analysis was conducted within a 300–900 nm wavelength range, scanning by the *Ae*-AgNPs.

#### 2.4.2. FTIR Analysis

The FTIR spectrum was obtained using infrared spectroscopy employing the Fourier transform and potassium bromide (KBr) pellets at room temperature [18]. A pellet was made by mixing the combination of *Ae*-AgNPs and KBr powder to investigate the biosynthesised *Ae*-AgNPs. The obtained spectra were then examined using a small FTIR spectrometer (Alpha II spectrometer, Bruker, Billerica, MA, USA) in the infrared (IR) range of 4000–400 cm<sup>-1</sup> [19].

#### 2.4.3. XRD Analysis

The crystal structure of *Ae*-AgNPs was characterised using the X-ray diffraction (XRD) technique [20]. Rigaku, Japan's Smart Lab 9 kW XRD equipment, was used to obtain the XRD pattern.

#### 2.4.4. Analysis of SEM and EDX

Using an SEM (JEOL, Japan, Tokyo) that runs at a voltage of 20 kV, SEM and EDX were performed. An EDX (OXFORD) detector fitted on SEM was utilised to determine the elemental composition of AgNPs.

### 2.5. Antioxidant Radical Scavenging Activity of *Ae*-AgNPs

#### 2.5.1. DPPH Assay

Using the DPPH free radical scavenging method and ascorbic acid as the positive control, the antioxidant strength of the *Ae*-AgNPs was evaluated [21]. Briefly, 2 mL of bio-synthesised AgNPs was diluted with water to obtain various concentrations (20–100 µg/mL). Then, 1 mL of DPPH solution (0.1 mM) was mixed with the diluted AgNPs solution [22]. The mixture was thoroughly mixed and stored in a dark room at room temperature. By measuring each sample's absorbance at 517 nm after a 30 min incubation period, the radical scavenging activity was ascertained.

#### 2.5.2. ABTS Assay

Using ABTS radical scavenging assay and ascorbic acid as the standard, the antioxidant strength of the *Ae*-AgNPs was determined [21]. Briefly, 100 µL of ABTS solution (triplicates) of varied (20–100 µg/mL) *Ae*-AgNP concentrations and equivalent amounts of ascorbic acid were combined [23]. At ambient temperature, each reaction mixture was left undisturbed for 20 min. Each reaction mixture had its absorbance measured at 734 nm.

#### 2.5.3. Hydrogen Peroxide (H<sub>2</sub>O<sub>2</sub>) Reducing Ability

The antioxidant potential of *Ae*-AgNPs was investigated under a previously established approach. A pH 7.4 phosphate-buffered solution was prepared to facilitate the

dissolution of hydrogen peroxide. Samples with varying concentrations (20–100 µg/mL) were mixed with 200 µL of each sample and 0.6 mL of the H<sub>2</sub>O<sub>2</sub> solution [24]. Hydrogen peroxide absorbance was measured at 230 nm using a UV-visible spectrophotometer. An inert solution (phosphate buffer alone, no hydrogen peroxide added) was used to establish a baseline absorbance value. Ascorbic acid was used as a reference compound at different concentrations.

## 2.6. Anti-Inflammatory Activity

### 2.6.1. Albumin Denaturation Assay

The potential mechanism of action was investigated by assessing the albumin denaturation inhibitory activity of both *Ae*-AgNPs and aspirin anti-inflammatory effects. Aspirin, a non-steroidal solid anti-inflammatory medicine, served as the comparator. Different sterile tubes containing 20–100 µg/mL of 1% aqueous bovine serum albumin (BSA) solution and 20–100 µg/mL of *Ae*-AgNPs in varied aliquots were subjected to incubation at a temperature of 37 °C for 20 min. After the incubation period, the tubes underwent heat treatment, inducing the denaturation of BSA by subjecting it to a water bath at 71 °C for 30 min [25]. After the tubes had cooled, the absorbance of the samples was assessed at 660 nm compared to a blank made up entirely of pure water. The study was performed three times, and the average absorption was computed.

### 2.6.2. Membrane Stabilisation Assay

To prepare the red blood cell (RBC) suspension, recently collected blood samples were collected from a healthy volunteer, and erythrocyte suspension was produced under the usual methodology [26,27]. The entire volume of the test solution was 2 mL, of which 1 mL was a 10% RBC suspension, and the remaining 1 mL was a heat-induced haemolysis prevention *Ae*-AgNPs. In the control sample, regular saline was used in place of *Ae*-AgNPs. As a standard drug in this case, aspirin was utilised at a concentration of 200 µg/mL [28]. Before being kept in a water bath, the tubes were set at 56 °C for half an hour, and the samples were thoroughly mixed by gently inverting them. After the incubation period, the reaction mixture was centrifuged at 37 °C at 2500 rpm. Under running water, the cooling tubes were used. The supernatant was gathered, and its absorbance at 560 nm was measured. The phosphorus buffer was treated as empty.

## 2.7. Anti-Diabetic Activity

### Inhibition of Proteinase Action

When dissolved in a 20 mM sodium phosphate buffer, the amount of *Ae*-AgNPs (20–100 µg/mL) that inhibited the activity of the enzymes α-amylase and α-glucosidase was evaluated [29]. The enzymes α-amylase and α-glucosidase were exposed to different quantities of *Ae*-AgNPs and incubated at 4 °C for 30 min. Subsequently, the enzyme activity of glucosidase and amylase was determined using the previously mentioned method. A typical drug called acarbose was used as a standard [21].

## 2.8. Antimicrobial Effect of *Ae*-AgNPs

Antimicrobial activity was investigated to determine the *Ae*-AgNPs. The antibacterial abilities of silver nanoparticles were tested using two fungal strains and ten different bacterial strains. The microbiology lab provided the bacterial strains for this study, including gram positive bacteria (*Bacillus subtilis*, *Enterococcus faecalis*, *Micrococcus luteus*, *Staphylococcus aureus*, and *Streptococcus pyogenes*), five gram negative strains of bacteria (*Escherichia coli*, *Salmonella typhi*, *Proteus vulgaris*, *Vibrio parahaemolytic*, and *Klebsiella pneumonia*), and two strains of fungus (*Candida albicans* and *Aspergillus niger*) [30]. The microbiology lab delivered the microbial strains. The Muller Hinton broth-based inoculum was prepared from freshly isolated cultures of bacteria. Chloramphenicol disc was used as a positive control. The Potato Dextrose Agar broth-based inoculum was prepared from freshly isolated cultures of the fungus, and 100 units of Fluconazole were used as a positive control.

To determine whether or not *Ae*-AgNPs were effective against the designated microorganisms, an agar well diffusion test [31] was used. Using the lawn culture method, a sterile cotton swab was used to apply the bacterial inoculum to the Muller–Hinton Agar (MHA) and fungal inoculum to the Potato Dextrose Agar (PDA). Immediately after the injection, using the backside blue micropipette tips, we created five wells in the agar plate. Two droplets of melted MHA agar were used to seal the bottom region of the wells after waiting 10 min for the melted agar to solidify. Then, in separate wells, four unique concentrations of *Ae*-AgNPs (25, 50, 75, and 100 µg/mL) were extracted from nanoparticles. Regarded as a valuable control for comparison. After that, the plates were maintained at 37 °C for 18 to 24 h.

### 2.9. Statistical Analysis

Statistical analysis was performed using SPSS 16 (SPSS, Inc., Chicago, IL, USA). The data are expressed as mean ± standard deviation (SD). One-way analysis of variance (ANOVA) followed by the Duncan Multiple Range Test (DMRT) comparison method was used to correlate the difference between the variables. Data are considered statistically significant if *p*-values are less than 0.05.

## 3. Results

### 3.1. Biosynthesised *Ae*-AgNPs

Aqueous extract from the plant *Ae* was used to biosynthesise silver nanoparticles. When the aqueous extract was added, the colour of the AgNO<sub>3</sub> became a brownish yellow, as shown in (Figure 1), indicating the preliminary production of *Ae*-AgNPs. The activation of free electrons in the nanoparticles causes a brownish-yellow tint, which develops after three hours at ambient temperature. No more colour change was seen after 24 h due to the stabilised manufactured nanoparticles.

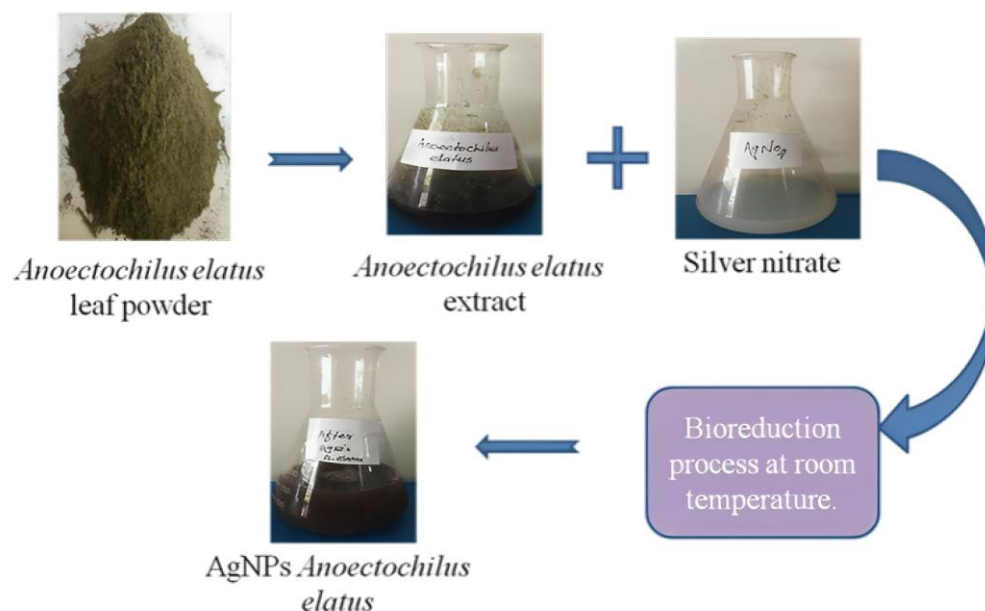


**Figure 1.** Synthesis of AgNPs using *Anoectochilus elatus* aqueous leaf extract.

### 3.2. Characterisation of *Ae*-AgNPs

UV-vis is a technique used for absorption spectroscopy in the UV-vis spectral range. In this region of the electromagnetic spectrum, molecules undergo electronic transitions (Figure 2), displaying the UV-vis spectrum of *Ae*-AgNPs. The change in the silver nanoparticles that were produced during the reduction in silver ions to silver nanoparticles that were mediated by plant extract. After 24 h of preparation, the absorption spectra of the *Ae*-AgNPs were measured, revealing an absorbance at 480 nm, which is indicative of silver nanoparticles.

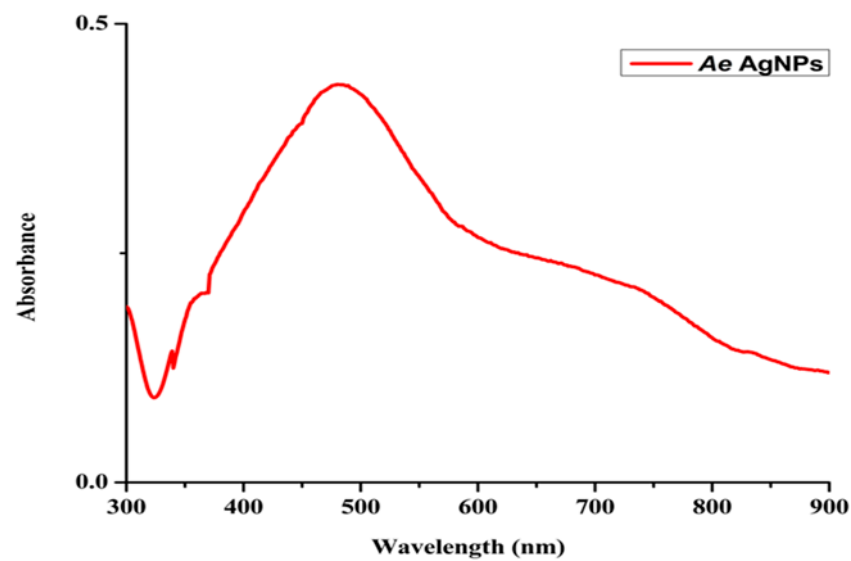


**Figure 2.** UV-VIS spectroscopy for AgNPs synthesised using *Anoectochilus elatus* leaves extracts.

The crystalline size of the green synthesised *Ae*-AgNPs was characterised by X-ray powder diffraction. (Figure 3) represents the XRD pattern of green synthesised *Ae*-AgNPs, the peaks at 32.44, 38.00, 44.11, 57.24, 64.36, and 77.38 were assigned to planes of (110), (111), (200), (121), (220), and (311), respectively. All the peaks are confirmed AgNP cubic phases; no more impurities were found in *Ae*-AgNPs. The Debye–Scherer formula ( $D = K^*/\text{Cos}\theta$ ) calculates the average particle size. *Ae*-AgNP average crystallite size is found to be approximately 22.52 nm.

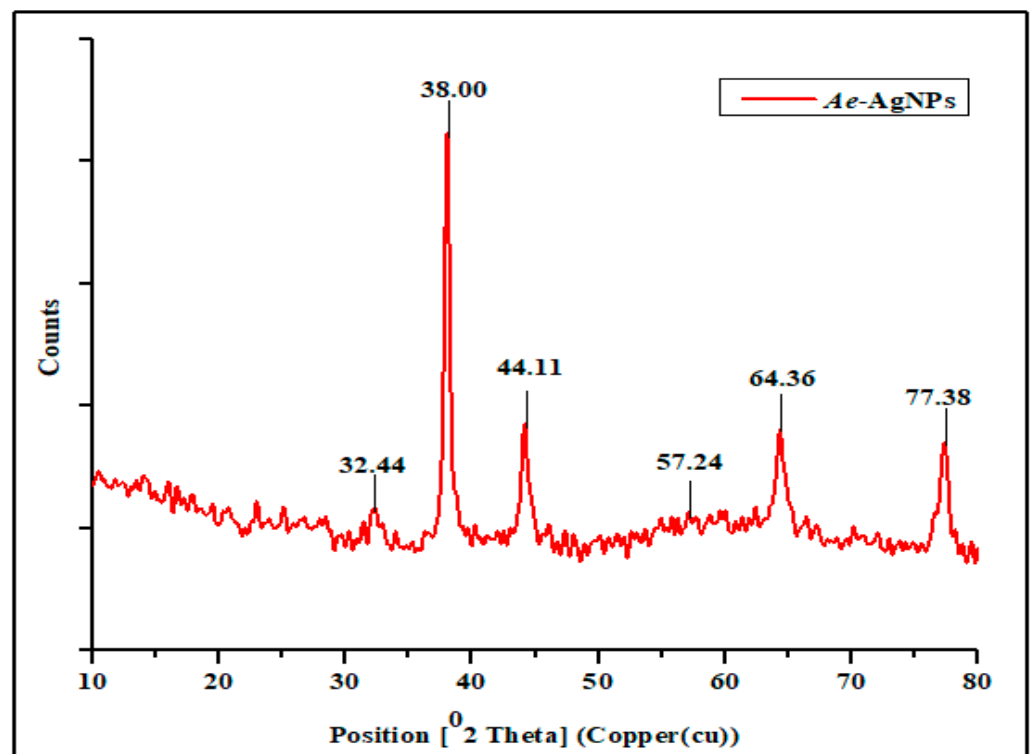


**Figure 3.** XRD pattern of the synthesised AgNPs using *Anoectochilus elatus* leaves extract.

The FTIR spectra of green synthesised *Ae*-AgNPs are shown in (Figure 4). The Fourier transform infrared spectroscopy was used to determine the existence of functional groups in the samples based on their vibrational (transmittance/absorption) spectra. The broad

band observed at  $3320\text{ cm}^{-1}$  corresponds to phenolic compounds O–H stretching. The C–H stretching vibrations presence was attributed to  $2918$  and  $2851\text{ cm}^{-1}$ , and the band at  $1731\text{ cm}^{-1}$  denotes the amines C–N stretching bonds. The amide C=O stretching corresponds to  $1625\text{ cm}^{-1}$ , and  $2113\text{ cm}^{-1}$  denotes the alkyne group present in the phytoconstituents of the extract. Peaks of  $1296$ ,  $1141$ , and  $810\text{ cm}^{-1}$  are attributed to the C–O stretch, –COC– linkages, and Ag groups, respectively.

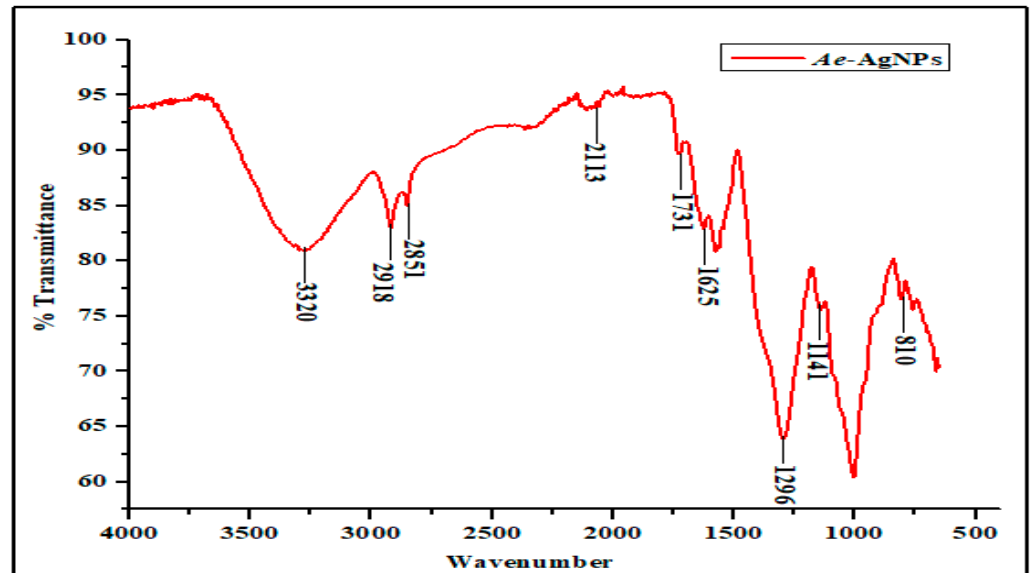


**Figure 4.** The FTIR spectrum presence of major functional groups in the AgNPs synthesised using the *Anoectochilus elatus* leaves extract.

SEM determined the morphology of the green synthesised *Ae*-AgNPs, shown in (Figure 5a). The SEM image shows the spherical shape, and these particles are highly agglomerated. The evident homogeneity of the particles indicates their presence in a uniform form, highlighting the significance of nanoparticle homogeneity in the various activities they exhibit. EDX spectrum (Figure 5b) shows peaks of silver, which reveals the presence of silver nanoparticles and oxide as impurities from the sample substrate. The EDX spectra investigate the composition and distribution of the *Ae*-AgNP elements.

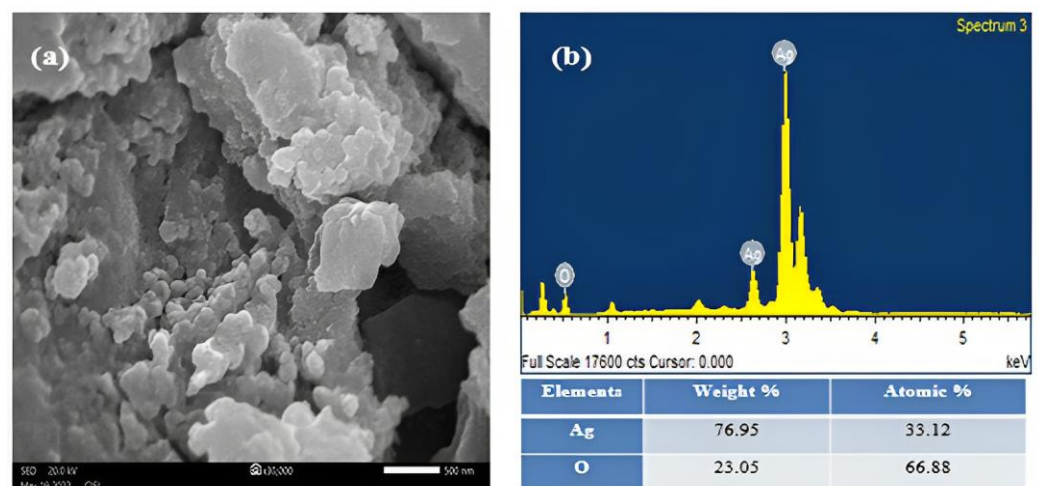


**Figure 5.** (a) SEM and (b) EDX images of AgNPs synthesised using the *Anoectochilus elatus* leaves extract.

### 3.3. Antioxidant Free Radical Scavenging Assay of DPPH, ABTS, and H<sub>2</sub>O<sub>2</sub>

The scavenging activity of free radicals in the DPPH, ABTS, and H<sub>2</sub>O<sub>2</sub> assays was dose-dependent. As the concentration of green synthesised *Ae*-AgNPs increased, the maximum free radical scavenging activities were recorded at 87.82% for all three assays (Figure 6a–c) at 100 µg/mL<sup>-1</sup>. Notably, this percentage closely resembled the scavenging activity of the positive control, ascorbic acid, which was 92.65%. The scavenging percentage of *Ae*-AgNPs was statistically significant compared to the control. The IC<sub>50</sub> values for the DPPH, ABTS, and H<sub>2</sub>O<sub>2</sub> assays of green synthesised *Ae*-AgNPs and standard ascorbic acid are shown in (Table 1).

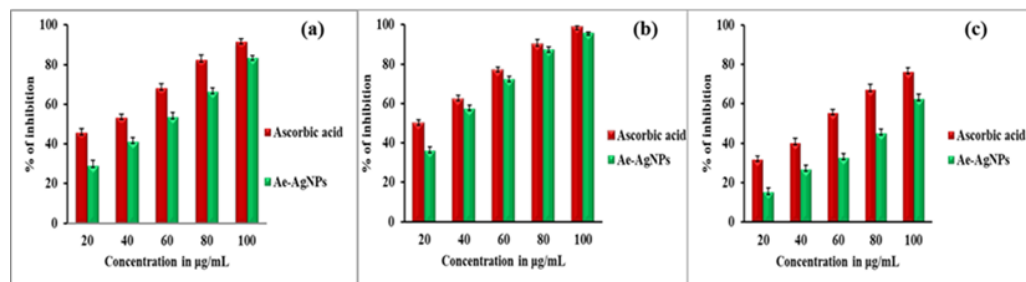


**Figure 6.** Graphical representation of the figure shows (a) DPPH, (b) ABTS, and (c) H<sub>2</sub>O<sub>2</sub> radical scavenging activity of *Ae*-AgNPs compared with standard drugs using different concentrations. All the values are the average of three replicates; error bars represent the standard errors of the means and the significant difference at  $p < 0.05$ .

**Table 1.** The IC<sub>50</sub> value of the Antioxidant radical scavenging assay indicated that values were significantly different at  $p \leq 0.05$ .

Antioxidant Radical Scavenging Assay	DPPH (µg/mL)	ABTS (µg/mL)	H <sub>2</sub> O <sub>2</sub> (µg/mL)
Standard IC <sub>50</sub> value	53 ± 0.09	33 ± 0.05	84 ± 0.19
<i>Ae</i> -AgNPs IC <sub>50</sub> value	30 ± 0.05	19 ± 0.03	53 ± 0.09

### 3.4. Anti-Inflammatory Activity of *Ae*-Ag NPs

Green synthesised *Ae*-AgNPs were examined in this research. At different doses, the ability of these nanoparticles to stop the breakdown of albumin and the stabilisation of membranes were compared to that of aspirin.

#### 3.4.1. Inhibition of Egg Albumin Denaturation

The results showed that increasing the concentration of green synthesised *Ae*-AgNPs and aspirin led to a significant increase in their inhibition of bovine serum albumin. This inhibition was concentration-dependent, as shown in (Figure 7a). The *Ae*-AgNPs and aspirin exhibited similar levels of inhibition, with percentages of 67.03 ± 2.22% and 79.11 ± 2.65%, respectively, at a 100 µg/mL concentration. At all studied quantities, the statistical analysis showed that *Ae*-AgNPs and aspirin were very different in their ability to stop albumin from breaking down. (Table 2) presents the IC<sub>50</sub> values for the albumin denaturation and membrane stabilisation assays of green synthesised *Ae*-AgNPs and aspirin.

**Table 2.** The IC<sub>50</sub> value of the anti-inflammatory assay indicated that values were significantly different at  $p \leq 0.05$ .

Anti-Inflammatory Assay	Albumin Denaturation (µg/mL)	Membrane Stabilisation (µg/mL)
Standard IC <sub>50</sub> value	68.82 ± 0.15	65.02 ± 0.14
<i>Ae</i> -AgNPs IC <sub>50</sub> value	47.28 ± 0.08	55.93 ± 0.12

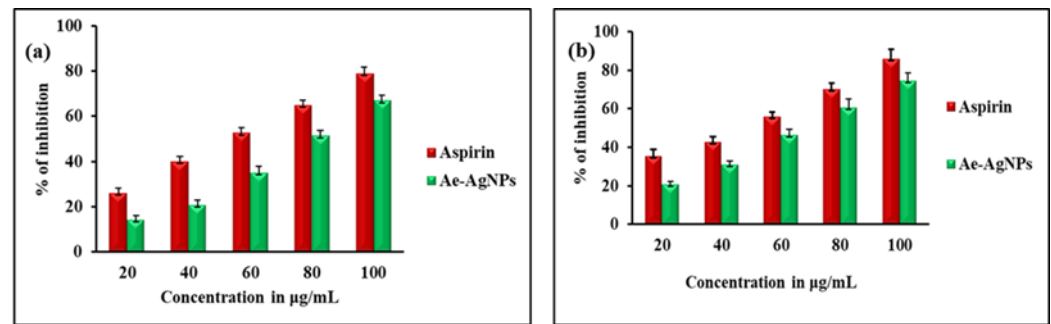


**Figure 7.** Graphical representation of the figure shows an (a) Albumin denaturation and (b) Membrane stabilisation activity of *Ae*-AgNPs compared with standard drugs using different concentrations. All the values are the average of three replicates; error bars represent the standard errors of the means and the significant difference at  $p < 0.05$ .

### 3.4.2. Membrane Stabilisation

Regarding membrane stabilisation, the *Ae*-AgNPs demonstrated percentages of  $14.24 \pm 1.90\%$  and  $74.39 \pm 4.12\%$  as the minimum and maximum activities, respectively, for human red blood cells. Similarly, aspirin exhibited a membrane stabilisation percentage of  $86.00 \pm 4.66\%$  at  $100 \mu\text{g/mL}$ . These results are depicted in (Figure 7b). The statistical analysis demonstrated a lack of significant difference  $p < 0.05$  observed in the percentage of membrane stabilisation between *Ae*-AgNPs and aspirin at any of the tested concentrations.

### 3.5. Antidiabetic Activity of *Ae*-Ag NPs

#### $\alpha$ -Amylase and $\alpha$ -Glucosidase Inhibition Assay

The present study investigated *Ae*-AgNPs with known antidiabetic activity for their potential to inhibit ( $\alpha$ -amylase and  $\alpha$ -glucosidase) activity was examined in this study. Different concentrations (20–100  $\mu\text{g/mL}$ ) of *Ae*-AgNPs were separately and synergistically tested for the  $\alpha$ -amylase and  $\alpha$ -glucosidase inhibitory activity (Figure 8a,b). The *Ae*-AgNPs, at  $100 \mu\text{g/mL}$  concentration, had the most significant Inhibition of  $74.03 \pm 3.92\%$  and  $82.00 \pm 3.57\%$ , while the standard had at  $86.40 \pm 2.08\%$  and  $94.47 \pm 4.09\%$ , amylase and glucosidase inhibition. The IC<sub>50</sub> values of *Ae*-AgNPs and acarbose are shown in (Table 3).

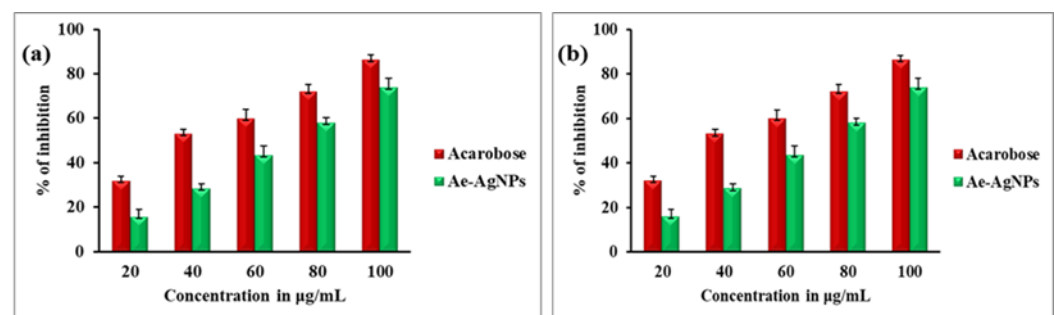


**Figure 8.** Graphical representation of the figure shows an (a)  $\alpha$ -Amylase and (b)  $\alpha$ -Glucosidase antidiabetic activity of *Ae*-AgNPs compared with standard drugs using different concentrations. All the values are the average of three replicates, error bars represent the standard errors of the means, and the significant difference at  $p < 0.05$ .

**Table 3.** The IC50 value of Antidiabetic Activity indicated that values were significantly different at  $p \leq 0.05$ .

Anti-Diabetic Activity	$\alpha$ -Amylase ( $\mu\text{g/mL}$ )	$\alpha$ -Glucosidase ( $\mu\text{g/mL}$ )
Standard IC50 value	68.23 $\pm$ 0.15	56.71 $\pm$ 0.10
<i>Ae</i> -AgNPs IC50 value	43.17 $\pm$ 0.07	29.80 $\pm$ 0.04

### 3.6. Antimicrobial Activity of *Ae*-AgNPs

*Ae*-AgNPs tested against the Gram-positive (*Staphylococcus aureus*, *Streptococcus pyogenes*, *Bacillus subtilis*, *Micrococcus luteus*, and *Enterococcus faecalis*) and Gram-negative (*Escherichia coli*, *Salmonella typhi*, *Proteus vulgaris*, *Klebsiella pneumoniae*, and *Vibrio parahaemolyticus*) and fungus (*Candida albicans* and *Aspergillus niger*). *Ae*-AgNPs exhibited potent antimicrobial efficacy against fungi and Gram-negative bacteria while demonstrating moderate activity against Gram-positive bacteria. Activities of *Ae*-AgNPs are summarised in (Table 4) and presented in (Figure 9a–c). Gram-positive and Gram-negative bacteria and fungus had the highest inhibition zones at a concentration of 100  $\mu\text{g/mL}$  with zone sizes of 22 mm, 23 mm, and 16 mm, respectively.

**Table 4.** Zone of inhibition of Gram-Positive and Gram-Negative bacteria and fungal using different concentrations of the aqueous leaf extract of *Ae*-AgNPs. Different letters in the same column indicated that values were significantly different at  $p \leq 0.05$ .

S. No	Microorganisms	Zone of Inhibition (MM)				Positive Control
		100	75	50	25	
<b>Gram positive bacteria</b>						
1	<i>Staphylococcus aureus</i>	20 $\pm$ 1.60 <sup>a</sup>	19 $\pm$ 1.52 <sup>b</sup>	16 $\pm$ 1.28 <sup>c</sup>	13 $\pm$ 1.04 <sup>d</sup>	24 $\pm$ 1.94 <sup>a</sup>
2	<i>Streptococcus pyogenes</i>	22 $\pm$ 1.76 <sup>a</sup>	20 $\pm$ 1.60 <sup>b</sup>	16 $\pm$ 1.28 <sup>c</sup>	12 $\pm$ 0.96 <sup>d</sup>	25 $\pm$ 2.00 <sup>a</sup>
3	<i>Bacillus subtilis</i>	19 $\pm$ 1.52 <sup>a</sup>	16 $\pm$ 1.28 <sup>b</sup>	15 $\pm$ 1.20 <sup>c</sup>	11 $\pm$ 0.88 <sup>d</sup>	23 $\pm$ 1.84 <sup>a</sup>
4	<i>Enterococcus faecalis</i>	20 $\pm$ 1.60 <sup>a</sup>	18 $\pm$ 1.44 <sup>b</sup>	13 $\pm$ 1.04 <sup>c</sup>	10 $\pm$ 0.80 <sup>d</sup>	24 $\pm$ 1.92 <sup>a</sup>
5	<i>Micrococcus luteus</i>	18 $\pm$ 1.44 <sup>a</sup>	15 $\pm$ 1.20 <sup>b</sup>	12 $\pm$ 0.96 <sup>c</sup>	11 $\pm$ 0.88 <sup>d</sup>	22 $\pm$ 1.76 <sup>a</sup>
<b>Gram negative bacteria</b>						
6	<i>E. coli</i>	23 $\pm$ 1.84 <sup>a</sup>	18 $\pm$ 1.44 <sup>b</sup>	17 $\pm$ 1.36 <sup>c</sup>	15 $\pm$ 1.20 <sup>d</sup>	24 $\pm$ 1.92 <sup>a</sup>
7	<i>Klebsiella pneumoniae</i>	17 $\pm$ 1.36 <sup>a</sup>	13 $\pm$ 1.04 <sup>b</sup>	11 $\pm$ 0.88 <sup>c</sup>	10 $\pm$ 0.80 <sup>d</sup>	22 $\pm$ 1.76 <sup>a</sup>
8	<i>Proteus vulgaris</i>	21 $\pm$ 1.68 <sup>a</sup>	18 $\pm$ 1.44 <sup>b</sup>	14 $\pm$ 1.12 <sup>c</sup>	11 $\pm$ 0.88 <sup>d</sup>	24 $\pm$ 1.92 <sup>a</sup>
9	<i>Salmonella typhi</i>	20 $\pm$ 1.60 <sup>a</sup>	17 $\pm$ 1.36 <sup>b</sup>	15 $\pm$ 1.20 <sup>c</sup>	13 $\pm$ 1.04 <sup>d</sup>	23 $\pm$ 1.84 <sup>a</sup>
10	<i>Vibrio parahaemolyticus</i>	18 $\pm$ 1.44 <sup>a</sup>	15 $\pm$ 1.20 <sup>b</sup>	12 $\pm$ 0.96 <sup>c</sup>	10 $\pm$ 0.80 <sup>d</sup>	24 $\pm$ 1.92 <sup>a</sup>
<b>Fungal</b>						
11	<i>Aspergillus niger</i>	14 $\pm$ 1.12 <sup>a</sup>	12 $\pm$ 0.96 <sup>b</sup>	09 $\pm$ 0.72 <sup>c</sup>	08 $\pm$ 0.63 <sup>d</sup>	20 $\pm$ 1.60 <sup>a</sup>
12	<i>Candida albicans</i>	16 $\pm$ 1.28 <sup>a</sup>	14 $\pm$ 1.12 <sup>b</sup>	12 $\pm$ 0.96 <sup>c</sup>	10 $\pm$ 0.80 <sup>d</sup>	23 $\pm$ 1.84 <sup>a</sup>

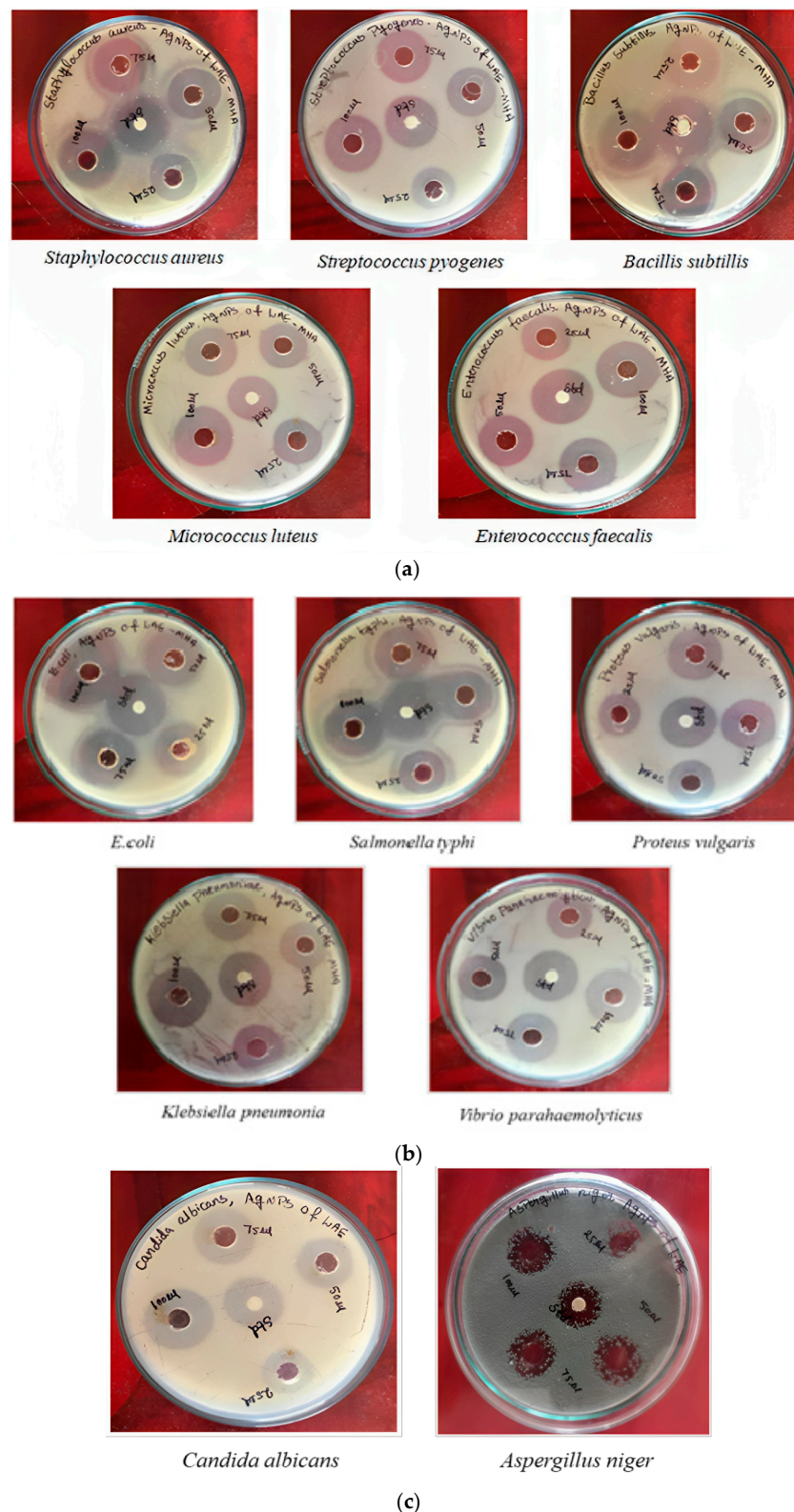


**Figure 9.** (a). Anti-bacterial activity tested plates of Gram-Positive bacteria *Staphylococcus aureus*, *Streptococcus pyogenes*, *Bacillus subtilis*, *Micrococcus luteus*, and *Enterococcus faecalis* of synthesised AgNPs from *Anoectochilus elatus* leaf extract. (b) Anti-bacterial activity tested plates of Gram-negative bacteria *E. coli*, *Salmonella typhi*, *Proteus vulgaris*, *Klebsiella pneumonia*, and *Vibrio parahaemolyticus* of synthesised AgNPs from *Anoectochilus elatus* leaf extract. (c) Anti-fungal activity tested plates of *Candida albicans* and *Aspergillus niger* of synthesised AgNPs from *Anoectochilus elatus* leaf extract.

#### 4. Discussion

The enormous potential of nanomaterials has gained the attention of numerous researchers around the world. Due to the huge interest in metallic nanoparticles, AgNPs are recognised for their characteristic aqueous solution exhibiting a yellowish-brown colour, which arises from the excitation of surface plasmon vibrations [32,33]. A brown colour in the reaction vessels indicates the formation of AgNPs.

According to [34], the UV absorption peak of AgNPs typically falls within the 300 to 900 nm range. The UV absorption peaks of *Ae*-AgNPs show clear peaks at approximately 480 nm. This observation confirms the formation of AgNPs in the plant extracts. This peak is at 480 nm and a shoulder at 720 nm, which shows the formation of anisotropic particles. In general, the number of SPR peaks increases as the symmetry of particles decreases. According to the Mie theory, small spherical nanocrystals of Ag and Au exhibit only a single SPR band, whereas anisotropic particles show 2–3 bands, depending on their shape. The peak at 427 nm is attributed to the transverse oscillation of electrons and has contributions from the light scattering as well. The SPR band in the form of a shoulder at 590 nm is attributed to the longitudinal oscillation of electrons, which can be shifted even up to 1000 nm in the near-IR region and has originated from anisotropic nanoparticles. Recent studies have also reported and indicated that silver nanoparticles are face-centred, cubic, and crystalline [35–38]. A similar type of result was also observed for the AgNPs synthesised using fruit extract of *B. retusa*. *Bridelia retusa* fruit synthesised AgNPs were FCC crystals with 22.48 nm size [39]. FTIR is a valuable technique used to analyse the involvement of functional groups in the interactions between metal particles and biomolecules. Our FTIR analysis shows the C–O stretch, –COC– linkages, and Ag groups [40–42]. The resulting AgNPs exhibit various shapes, including cubical, rectangular, triangular, and spherical, with a uniform distribution [43]. The EDX spectra investigate the composition and distribution of the AgNP elements.

Antioxidant activity is a crucial property of nanoparticles that can significantly against oxidative damage. The antioxidant activity of green synthesised silver nanoparticles can be evaluated using several assays, including DPPH, ABTS, and H<sub>2</sub>O<sub>2</sub> scavenging assays. The antioxidant activity of green synthesised silver nanoparticles in these assays can be attributed to several factors. To begin, the phytochemical components that are found in plant extracts that are used in the production of nanoparticles have the potential to contribute to the antioxidant activity of the final product. These constituents, such as polyphenols, flavonoids, and other bioactive compounds, possess inherent antioxidant properties. Second, the nanoparticles may exhibit unique physicochemical properties that enhance their antioxidant capacity. The high surface area-to-volume ratio of nanoparticles allows for increased interactions with free radicals, leading to effective scavenging. Additionally, silver nanoparticles' small size and unique electronic properties may facilitate electron transfer or radical quenching, further enhancing their antioxidant potential. *A. aestivus* silver nanoparticles showed antioxidant activity in DPPH, ABTS, and H<sub>2</sub>O<sub>2</sub> scavenging assays [44].

Studies have shown silver nanoparticles can bind to albumin and induce conformational changes, leading to denaturation. This can be attributed to the strong affinity of silver nanoparticles for proteins and their ability to disrupt the hydrogen bonding and hydrophobic interactions that stabilise the protein structure. The oxidative stress generated by silver nanoparticles can also contribute to protein denaturation. In our study, we noticed that AgNPs denature protein, which matches with a previous study conducted by [45,46].

Silver nanoparticle stabilisation of cell membranes can be attributed to several factors. Firstly, silver nanoparticles can interact with the lipid molecules in the membrane, forming a protective layer that reduces membrane disruption. Secondly, they can scavenge reactive oxygen species (ROS) generated during oxidative stress, thereby reducing membrane damage. Finally, silver nanoparticles can modulate membrane-associated enzymes and signalling pathways, contributing to membrane stabilisation. AgNPs synthesised using *Calophyllum tomentosum* leaf extract had strong membrane stabilisation activity [47].

$\alpha$ -Amylase is an enzyme responsible for breaking down complex carbohydrates into simpler sugars such as glucose. Inhibitions of  $\alpha$ -amylase activity can reduce the rate at which carbohydrates are broken down into glucose, leading to a slower release of glucose into the bloodstream after a meal. Green synthesised AgNPs have been investigated for their inhibitory effect on  $\alpha$ -amylase activity. When exposed to  $\alpha$ -amylase, the nanoparticles can bind to the enzyme and prevent its proper functioning, thereby reducing the breakdown of carbohydrates and the subsequent release of glucose.  $\alpha$ -Glucosidase is another enzyme involved in carbohydrate digestion [48,49]. It is responsible for breaking down complex sugars (such as disaccharides) into simple sugars (such as glucose) that can be absorbed into the bloodstream. Inhibiting  $\alpha$ -glucosidase activity can slow down the conversion of complex sugars into glucose, reducing the rate of glucose absorption in the intestines. Green synthesised *Ae*-AgNPs have also been explored for their inhibitory effect on  $\alpha$ -glucosidase activity. These nanoparticles can interact with  $\alpha$ -glucosidase, interfering with its enzymatic activity and decreasing the conversion of complex sugars into glucose.

By inhibiting  $\alpha$ -glucosidase and  $\alpha$ -amylase enzymes, green synthesised silver nanoparticles can potentially help regulate blood sugar levels by reducing the rate of carbohydrate digestion and glucose absorption [50]. This property makes them promising candidates for developing natural and eco-friendly antidiabetic agents. According to the [51] study, AgNPs synthesised using *Lonicera japonica* leaf extract showed inhibition activity of  $\alpha$ -amylase and  $\alpha$ -glucosidase.

The antimicrobial properties of green synthesised silver nanoparticles are attributed to their unique characteristics. The small size and large surface area of these nanoparticles facilitate their interaction with microorganisms, leading to cellular damage and inhibition of microbial growth. They can disrupt the cell membrane, interfere with cellular processes, and induce oxidative stress, ultimately resulting in the death of the microorganisms. Moreover, green synthesis methods ensure the production of nanoparticles with well-defined shapes, sizes, and surface charges, enhancing their antimicrobial effectiveness [52]. Using natural reducing agents from plants or microorganisms can introduce additional antimicrobial compounds into the synthesis process, synergistically enhancing the overall antimicrobial activity of the nanoparticles [53]. A recent study reported varying inhibition zone diameters resulting from the antimicrobial activity of AgNPs against different bacteria. When testing AgNPs against negative strains, the found inhibition zones were 28.2 mm, 23.2 mm, 27.2 mm, and 28.4 mm [54].

## 5. Conclusions

The current investigation employed a biological approach to produce silver nanoparticles by dissolving silver nitrate in an aqueous leaf extract from *Anoectochilus elatus*. A UV-visible spectroscopy investigation found a peak at 480 nm that confirms the synthesised silver nanoparticles. SEM analysis showed that the synthesised AgNPs have the shape of a spherical. Based on the results of this study, the synthesised *Ae*-AgNPs have a wide range of antibacterial, antioxidant, anti-inflammatory, and antidiabetic properties. The DPPH, ABTS, and  $H_2O_2$  scavenging assays showed that the *Ae*-AgNPs had antioxidant activity. At 100  $\mu$ g/mL, *Ae*-AgNPs had the best antioxidant activity of the three doses because they could eliminate the free radicals. *Ae*-AgNPs were successful in killing bactericidal and fungicidal across all tested concentrations. At 100  $\mu$ g/mL, *Ae*-AgNPs had the most significant effect against pathogens. The right amount of *Ae*-AgNPs to fight free radicals and infections was 100  $\mu$ g/mL. According to the findings, *Ae*-AgNPs may act as antioxidants, antibiotics, and a preventative for infectious and non-infectious disorders. They will be used in the future since they are safe, affordable, and efficient. Further work is necessary to elucidate in detail the mechanism of action of *Ae*-AgNPs at the cellular and molecular levels.

**Author Contributions:** Conceptualisation, B.V.K. and N.V.; Data curation, R.M. and K.B.; Formal analysis, A.R.; Investigation, B.V.K., R.P. and R.G.; Methodology, B.V.K., B.R.A., R.P., C.K. and R.G.; Writing—original draft, B.V.K.; Writing—review and editing, N.V. and S.V. All authors have read and agreed to the published version of the manuscript.

**Funding:** The research work was funded by the Rashtriya Uchchar Shiksha Abhiyan 2.0 project grant (RUSA 2.0-100-E-002), Annamalai University, Tamil Nadu, India.

**Data Availability Statement:** The information provided in this research is accessible upon request from the corresponding author.

**Acknowledgments:** The authors are grateful for funding from the Rashtriya Uchchar Shiksha Abhiyan 2.0 project grant (RUSA 2.0-100-E-002), Annamalai University, Tamil Nadu, India.

**Conflicts of Interest:** The authors declare no conflict of interest.

## References

1. Sherif, N.A.; Kumar, T.S.; Rao, M.V. In vitro regeneration by callus culture of *Anoectochilus elatus* Lindley, an endangered terrestrial jewel orchid. *Vitr. Cell. Dev. Biol.* **2016**, *52*, 72–80. [[CrossRef](#)]
2. Prasad, K.; Karuppusamy, S.; Pullaiah, T. *Orchids of Eastern Ghats (India)*; Scientific Publishers: Jodhpur, India, 2019.
3. Mohapatra, P.; Ray, A.; Jena, S. Evaluation of Genetic Stability of In Vitro Raised Orchids Using Molecular-Based Markers. In *Commercial Scale Tissue Culture for Horticulture and Plantation Crops*; Springer: Singapore, 2022; Volume 17, pp. 293–316.
4. Vijayakumar, N.; Bhuvaneshwari, V.K.; Ayyadurai, G.K.; Jayaprakash, R.; Gopinath, K.; Nicoletti, M.; Alarifi, S.; Govindarajan, M. Green synthesis of zinc oxide nanoparticles using *Anoectochilus elatus*, and their biomedical applications. *Saudi J. Biol. Sci.* **2022**, *4*, 2270–2279. [[CrossRef](#)] [[PubMed](#)]
5. Wu, Y.B.; Peng, M.C.; Zhang, C.; Wu, J.G.; Ye, B.Z.; Yi, J.; Wu, J.Z.; Zheng, C.J. Quantitative determination of multi-class bioactive constituents for quality assessment of ten *Anoectochilus*, four *Goodyera* and one *Ludisia* species in China. *Chin. Herb. Med.* **2020**, *12*, 430–439. [[CrossRef](#)] [[PubMed](#)]
6. Fatahi, M.; Anghelescu, N.E.; Vafaei, Y.; Khoddamzadeh, A. Micropropagation of *Dactylorhiza umbrosa* (Kar. & Kir.) Nevski through asymbiotic seed germination and somatic embryogenesis: A promising tool for conservation of rare terrestrial orchids. *S. Afr. J. Bot.* **2023**, *159*, 492–506.
7. Gantait, S.; Das, A.; Mitra, M.; Chen, J.T. Secondary metabolites in orchids: Biosynthesis, medicinal uses, and biotechnology. *S. Afr. J. Bot.* **2021**, *139*, 338–351. [[CrossRef](#)]
8. Al-Khattaf, F.S. Gold and silver nanoparticles: Green synthesis, microbes, mechanism, factors, plant disease management and environmental risks. *Saudi J. Biol. Sci.* **2021**, *28*, 3624–3631. [[CrossRef](#)]
9. Gauba, A.; Hari, S.K.; Ramamoorthy, V.; Vellasamy, S.; Govindan, G.; Arasu, M.V. The versatility of green synthesized zinc oxide nanoparticles in sustainable agriculture: A review on metal-microbe interaction that rewards agriculture. *Physiol. Mol. Plant Pathol.* **2023**, *13*, 102023. [[CrossRef](#)]
10. Gregory, D.A.; Tripathi, L.; Fricker, A.T.; Asare, E.; Orlando, I.; Raghavendran, V.; Roy, I. Bacterial cellulose: A smart biomaterial with diverse applications. *Mater. Sci. Eng. R. Rep.* **2021**, *145*, 100623. [[CrossRef](#)]
11. Virkutyte, J.; Varma, R.S. Green synthesis of metal nanoparticles: Biodegradable polymers and enzymes in stabilization and surface functionalization. *Chem. Sci.* **2011**, *5*, 837–846. [[CrossRef](#)]
12. Kummara, S.; Patil, M.B.; Uriah, T. Synthesis, characterization, biocompatible and anticancer activity of green and chemically synthesized silver nanoparticles—A comparative study. *Biomed. Pharmacother.* **2016**, *84*, 10–21. [[CrossRef](#)]
13. Jubair, N.; Rajagopal, M.; Chinnappan, S.; Abdullah, N.B.; Fatima, A. Review on the antibacterial mechanism of plant-derived compounds against multidrug-resistant bacteria (MDR). *Evid.-Based Complement. Altern. Med.* **2021**, *2021*, 3663315. [[CrossRef](#)] [[PubMed](#)]
14. Gupta, A.; Vedula, S.; Srivastava, R.; Tamoli, S.; Mundhe, N.; Wagh, D.N.; Batra, S.; Patil, M.; Pawar, H.B.; Rai, R.K. Prospective, randomized, open-label, blinded endpoint, two-arm, comparative clinical study to evaluate the efficacy and safety of a fixed Ayurvedic regimen (FAR) as add-on to conventional treatment in the management of mild and moderate COVID-19 patients. *J. Pharm. Bioallied Sci.* **2021**, *2*, 256.
15. Riaz, M.; Sharafat, U.; Zahid, N.; Ismail, M.; Park, J.; Ahmad, B.; Rashid, N.; Fahim, M.; Imran, M.; Tabassum, A. Synthesis of biogenic silver nanocatalyst and their antibacterial and organic pollutants reduction ability. *ACS Omega* **2022**, *17*, 14723–14734. [[CrossRef](#)] [[PubMed](#)]
16. Mbaebie, B.O.; Edeoga, H.O.; Afolayan, A.J. Phytochemical analysis and antioxidants activities of aqueous stem bark extract of *Schotia latifolia* Jacq. *Asian Pac. J. Trop. Biomed.* **2012**, *2*, 118–124. [[CrossRef](#)] [[PubMed](#)]
17. Chi, N.T.; Narayanan, M.; Chinnathambi, A.; Govindasamy, C.; Subramani, B.; Brindhadevi, K.; Pimpimon, T.; Pikulkaew, S. Fabrication, characterization, anti-inflammatory, and anti-diabetic activity of silver nanoparticles synthesized from *Azadirachta indica* kernel aqueous extract. *Environ. Res.* **2022**, *208*, 112684.
18. Mulready, K.J.; McGoldrick, D. The establishment of a standard and real patient kidney stone library utilizing Fourier transform-infrared spectroscopy with a diamond ATR accessory. *Urol. Res.* **2012**, *40*, 483–498. [[CrossRef](#)]

19. Bajrami, D.; Fischer, S.; Barth, H.; Sarquis, M.A.; Ladero, V.M.; Fernández, M.; Sportelli, M.C.; Cioffi, N.; Kranz, C.; Mizaikoff, B. In situ monitoring of *Lentilactobacillus parabuchneri* biofilm formation via real-time infrared spectroscopy. *Npj Biofilms Microbiomes* **2022**, *1*, 92. [[CrossRef](#)]
20. Dua, T.K.; Giri, S.; Nandi, G.; Sahu, R.; Shaw, T.K.; Paul, P. Green synthesis of silver nanoparticles using *Eupatorium adenophorum* leaf extract: Characterizations, antioxidant, antibacterial and photocatalytic activities. *Chem. Pap.* **2023**, *77*, 2947–2956. [[CrossRef](#)]
21. Amalan, V.; Vijayakumar, N.; Ramakrishnan, A. p-Coumaric acid regulates blood glucose and antioxidant levels in streptozotocin-induced diabetic rats. *J. Chem. Pharm. Res.* **2015**, *7*, 831–839.
22. Sivaselvi, D.; Vijayakumar, N.; Jayaprakash, R.; Amalan, V.; Rajeswari, R.; Nagesh, M.R. Biocatalytic effect of *Simarouba glauca* leaf phytochemicals on biologically active silver nanoparticles yield and abts antioxidant activity: Green synthesis. *Rasayan J. Chem.* **2022**, *2*, 1166–1173. [[CrossRef](#)]
23. Venkatesan, A.; Vinoth Raja Antony Samy, J.; Balakrishnan, K.; Natesan, V.; Kim, S.J. In vitro antioxidant, anti-inflammatory, antimicrobial, and antidiabetic activities of synthesized chitosan-loaded p-Coumaric acid nanoparticles. *Curr. Pharm. Biotechnol.* **2023**, *9*, 1178–1194. [[CrossRef](#)] [[PubMed](#)]
24. Mishra, S.K.; Sinha, S.; Singh, A.K.; Upadhyay, P.; Kalra, D.; Kumar, P.; Tiwari, K.N.; Singh, R.; Singh, R.K.; Kumar, A.; et al. Green Synthesis, Characterization, and Application of *Ascophyllum nodosum* Silver Nanoparticles. *Regen. Eng. Transl. Med.* **2023**, *7*, 1–5. [[CrossRef](#)]
25. Radovanović, K.; Gavarić, N.; Aćimović, M. Anti-Inflammatory Properties of Plants from Serbian Traditional Medicine. *Life* **2023**, *4*, 874. [[CrossRef](#)] [[PubMed](#)]
26. Gul, A.; Ahmed, D.; Fazil, M.M.; Aslam, T.; Rashid, M.A.; Khan, H.; Ali, A.; Ali, S. Biofabrication of silver nanoparticles using *Spirulina platensis*: In vitro anti-coagulant, thrombolytic and catalytic dye degradation activity. *Microsc. Res. Tech.* **2023**, *26*, 823–833. [[CrossRef](#)] [[PubMed](#)]
27. Giridasappa, A.; Shareef, M.I.; Gopinath, S.M.; Rangappa, D.; Shivaramu, P.D.; Sabbanahalli, C. Synthesis, Antioxidant, Bactericidal and Antihemolytic Activity of Al<sub>2</sub>O<sub>3</sub> and SnO<sub>2</sub> Nanoparticles. *Proc. Natl. Acad. Sci. India Sect. B Biol. Sci.* **2023**, *10*, 1–2. [[CrossRef](#)]
28. Nwankwo, N.E.; Okeke, E.S.; Nworah, F.N.; Ezeako, E.C. Phytochemical composition and potential anti-inflammatory and antioxidant mechanisms of leaf extracts of *Sida linifolia* L. (Malvaceae). *J. Herb. Med.* **2023**, *38*, 100630. [[CrossRef](#)]
29. Kabach, I.; Bouchmaa, N.; Zouaoui, Z.; Ennoury, A.; El Asri, S.; Laabar, A.; Oumeslakht, L.; Cacciola, F.; El Majdoub, Y.O.; Mondello, L.; et al. Phytochemical profile and antioxidant capacity,  $\alpha$ -amylase and  $\alpha$ -glucosidase inhibitory activities of *Oxalis pes-caprae* extracts in alloxan-induced diabetic mice. *Biomed. Pharmacother.* **2023**, *160*, 114393. [[CrossRef](#)]
30. Chattopadhyay, A.; Das, N.; Banerjee, D. Mechanism of action of the lantibiotics on the multidrug-resistant organisms. In *Lantibiotics as Alternative Therapeutics*; Academic Press: Cambridge, MA, USA, 2023; Volume 1, pp. 85–117.
31. Ti, A.; Ej, I.; Adebayo, A.H. Evaluation of antioxidant and antimicrobial properties of silver nanoparticles biosynthesized using weed (*Dactyloctenium aegyptium*) extracts for sustainable environment, agriculture and ethnomedicine. *Mater. Today Proc.* **2023**, *7*, 1001–1014. [[CrossRef](#)]
32. Sivakumar, S.; Subban, M.; Chinnasamy, R.; Chinnaperumal, K.; Nakouti, I.; El-Sheikh, M.A.; Shaik, J.P. Green synthesized silver nanoparticles using *Andrographis macrobotrys* Nees leaf extract and its potential to antibacterial, antioxidant, anti-inflammatory and lung cancer cells cytotoxicity effects. *Inorg. Chem. Commun.* **2023**, *153*, 110787. [[CrossRef](#)]
33. Rajeshkumar, S.; Tharani, M.; Rajeswari, V.D.; Alharbi, N.S.; Kadaikunnan, S.; Khaled, J.M.; Gopinath, K.; Vijayakumar, N.; Govindarajan, M. Synthesis of greener silver nanoparticle-based chitosan nanocomposites and their potential antimicrobial activity against oral pathogens. *Green Process. Synth.* **2021**, *10*, 658–665. [[CrossRef](#)]
34. Ramteke, A.V.; Bhatia, D.; Pant, K.K. Conversion of light cycle oil to benzene and alkylated monoaromatics over monometallic and bimetallic CoMo catalysts in the presence of hydrogen donor. *Fuel* **2023**, *342*, 127737. [[CrossRef](#)]
35. Sahay, A.; Tomar, R.S.; Shrivastava, V.; Chauhan, P.S. Eugenol Loaded Ag-Ti-Co Nanocomposite as a Promising Antimicrobial and Antioxidative Agent. *BioNanoScience* **2023**, *2*, 339–351. [[CrossRef](#)]
36. Singh, S.; Bharti, A.; Meena, V.K. Green synthesis of multi-shaped silver nanoparticles: Optical, morphological and antibacterial properties. *J. Mater. Sci. Mater. Electron.* **2015**, *6*, 3638–3648. [[CrossRef](#)]
37. Paramelle, D.; Sadovoy, A.; Gorelik, S.; Free, P.; Hopley, J.; Fernig, D.G. A rapid method to estimate the concentration of citrate capped silver nanoparticles from UV-visible light spectra. *Analyst* **2014**, *139*, 4855–4861. [[CrossRef](#)] [[PubMed](#)]
38. Mogensen, K.B.; Kneipp, K. Size-dependent shifts of plasmon resonance in silver nanoparticle films using controlled dissolution: Monitoring the onset of surface screening effects. *J. Phys. Chem. C* **2014**, *48*, 28075–28083. [[CrossRef](#)]
39. Reddy, N.V.; Satyanarayana, B.M.; Sivasankar, S.; Pragathi, D.; Subbaiah, K.V.; Vijaya, T. Eco-friendly synthesis of silver nanoparticles using leaf extract of *Flemingia wightiana*: Spectral characterization, antioxidant and anticancer activity studies. *SN Appl. Sci.* **2020**, *2*, 1–10. [[CrossRef](#)]
40. El-Mehdawy, A. Green synthesis of silver nanoparticles using chitosan extracted from *Penaeus indicus* and its potential activity as aquatic larvicidal agent of *Culex pipens*. *Egypt. J. Aquat. Biol. Fish.* **2022**, *1*, 425–742. [[CrossRef](#)]
41. Tabatabaei, R.H.; Jafari, S.M.; Mirzaei, H.; Nafchi, A.M.; Dehnad, D. Preparation and characterization of nano-SiO<sub>2</sub> reinforced gelatin-k-carrageenan biocomposites. *Int. J. Biol. Macromol.* **2018**, *111*, 1091–1099. [[CrossRef](#)]
42. Dawadi, S.; Katuwal, S.; Gupta, A.; Lamichhane, U.; Thapa, R.; Jaisi, S.; Lamichhane, G.; Bhattarai, D.P.; Parajuli, N. Current research on silver nanoparticles: Synthesis, characterization, and applications. *J. Nanomater.* **2021**, *2021*, 6687290. [[CrossRef](#)]

43. Katta, V.K.; Dubey, R.S. Green synthesis of silver nanoparticles using *Tagetes erecta* plant and investigation of their structural, optical, chemical and morphological properties. *Mater. Today Proc.* **2021**, *45*, 794–798. [[CrossRef](#)]
44. Fafal, T.U.; Taştan, P.E.; Tüzün, B.S.; Ozyazici, M.; Kivcak, B. Synthesis, characterization and studies on antioxidant activity of silver nanoparticles using *Asphodelus aestivus* Brot. aerial part extract. *S. Afr. J. Bot.* **2017**, *112*, 346–353. [[CrossRef](#)]
45. Pretsch, A.; Nagl, M.; Schwendinger, K.; Kreiseder, B.; Wiederstein, M.; Pretsch, D.; Genov, M.; Hollaus, R.; Zinssmeister, D.; Debbab, A.; et al. Antimicrobial and anti-inflammatory activities of endophytic fungi *Talaromyces wortmannii* extracts against acne-inducing bacteria. *PLoS ONE* **2014**, *6*, e97929. [[CrossRef](#)] [[PubMed](#)]
46. Naz, R.; Ayub, H.; Nawaz, S.; Islam, Z.U.; Yasmin, T.; Bano, A.; Wakeel, A.; Zia, S.; Roberts, T.H. Antimicrobial activity, toxicity and anti-inflammatory potential of methanolic extracts of four ethnomedicinal plant species from Punjab, Pakistan. *BMC Complement. Altern. Med.* **2017**, *17*, 1–13. [[CrossRef](#)] [[PubMed](#)]
47. Govindappa, M.; Hemashekhar, B.; Arthikala, M.K.; Rai, V.; Ramachandra, Y.L. Characterization, antibacterial, antioxidant, antidiabetic, anti-inflammatory and antityrosinase activity of green synthesized silver nanoparticles using *Calophyllum tomentosum* leaves extract. *Results Phys.* **2018**, *9*, 400–408. [[CrossRef](#)]
48. Indyk, D.; Bronowicka-Szydełko, A.; Gamian, A.; Kuzan, A. Advanced glycation end products and their receptors in serum of patients with type 2 diabetes. *Sci. Rep.* **2021**, *1*, 13264. [[CrossRef](#)] [[PubMed](#)]
49. Oliveira, H.C.; Seabra, A.B.; Kondak, S.; Adedokun, O.P.; Kolbert, Z. Multilevel approach to plant–nanomaterial relationships: From cells to living ecosystems. *J. Exp. Bot.* **2023**, *22*, 107. [[CrossRef](#)]
50. Magaji, U.F.; Sacan, O.; Yanardag, R. Alpha amylase, alpha glucosidase and glycation inhibitory activity of *Moringa oleifera* extracts. *S. Afr. J. Bot.* **2020**, *128*, 225–230. [[CrossRef](#)]
51. Balan, K.; Qing, W.; Wang, Y.; Liu, X.; Palvannan, T.; Wang, Y.; Ma, F.; Zhang, Y. Antidiabetic activity of silver nanoparticles from green synthesis using *Lonicera japonica* leaf extract. *Rsc Adv.* **2016**, *46*, 40162–40168. [[CrossRef](#)]
52. Wang, L.; Hu, C.; Shao, L. The antimicrobial activity of nanoparticles: Present situation and prospects for the future. *Int. J. Nanomed.* **2017**, *14*, 1227–12249. [[CrossRef](#)]
53. Elemike, E.E.; Onwudiwe, D.C.; Saiyed, T.; Ekennia, A.C.; Azeez, M.A. Facile and green route to silver nanoparticles using aqueous plant extract, and their photocatalytic and antibacterial studies. *Mater. Sci.* **2020**, *4*, 489–4897. [[CrossRef](#)]
54. Said, A.; Abu-Elghait, M.; Atta, H.M.; Salem, S.S. Antibacterial activity of green synthesized silver nanoparticles using *Lawsonia inermis* against common pathogens from urinary tract infection. *Appl. Biochem. Biotechnol.* **2023**, 261–264. [[CrossRef](#)] [[PubMed](#)]

**Disclaimer/Publisher’s Note:** The statements, opinions and data contained in all publications are solely those of the individual author(s) and contributor(s) and not of MDPI and/or the editor(s). MDPI and/or the editor(s) disclaim responsibility for any injury to people or property resulting from any ideas, methods, instructions or products referred to in the content.